

***PENETRATION OF POLYMERIC NANOPARTICLES LOADED WITH AN HIV-1 INHIBITOR PEPTIDE DERIVED FROM GB VIRUS C IN A VAGINAL MUCOSA MODEL***

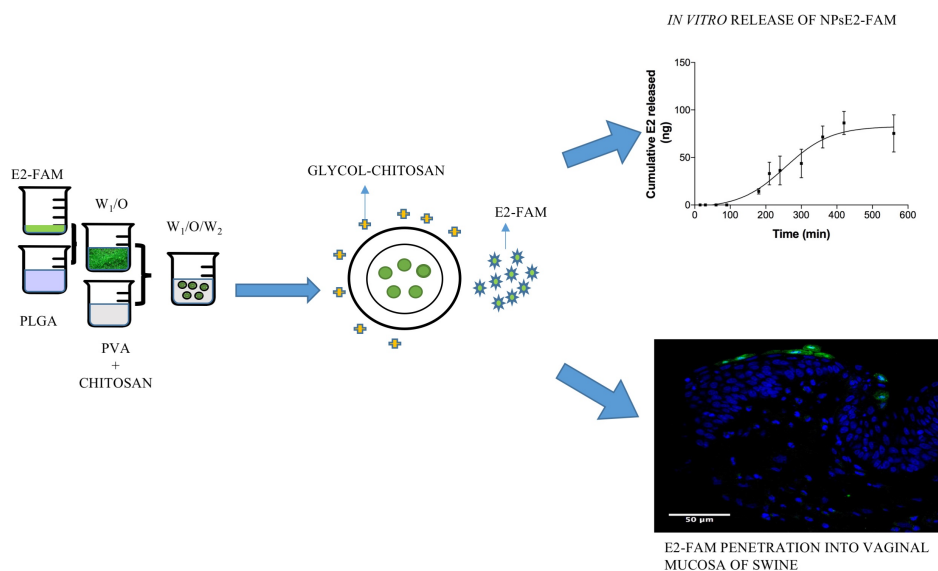
Martha Ariza-Sáenz<sup>a,b,\*</sup>, Marta Espina<sup>a</sup>, Nuria Bolaños<sup>c</sup>, Ana Cristina Calpena<sup>a</sup>, María José Gomara<sup>b</sup>, Isabel Haro<sup>b</sup>, María Luisa García<sup>a</sup>

<sup>a</sup>Department of Pharmacy and Pharmaceutical Technology and Physical Chemistry, University of Barcelona,

Av. Joan XXIII, 27-31, Barcelona 08028, Spain

<sup>b</sup>Unit of Synthesis and Biomedical Application of Peptides, Department of Biomedical Chemistry, IQAC-CSIC, Jordi Girona 18, 08034 Barcelona, Spain

<sup>c</sup>Laboratory of Experimental Nephrology, Department of Medicine, University of Barcelona, L'Hospitalet, Barcelona, Spain



**ABSTRACT**

Despite the great effort to decrease the HIV infectivity rate, current antiretroviral therapy has several weaknesses; poor bioavailability, development of drug resistance and poor ability to access tissues. However, molecules such as peptides have been regarded as a new strategy for HIV eradication. The vaginal mucosa is the main spreading point of HIV. There are natural barriers such as the vaginal fluid, which protects the vaginal epithelium from foreign agents. Here we developed and characterized nanoparticles (NPs) coated with glycol chitosan (GC), loaded with an HIV-1

inhibitor peptide (E2). *In vitro* release and *ex vivo* studies were carried out using the vaginal mucosa of swine, and the peptide was determined by HPLC MS/MS. Moreover, the peptide was labelled with 5(6)-carboxyfluorescein and entrapped in the NPs for studies *in vivo* to examine the penetration and toxicity of the NPs in the vaginal mucosa of swine. The mean size of the NPs, Z potential and the loading percentage were critical to determining whether the NPs reach the vaginal tissue and release the peptide within intercellular space. The results indicate that the fusion inhibitor peptides loaded into the NPs coated with GC might lead to the development of new treatment to prevent the transmission of HIV-1, since this formulation may be able to reach the human epithelial mucosa and release peptide without any side effects.

*Key words: Fusion inhibitor peptide; Polymeric Nanoparticles; In vitro peptide release; in vivo and ex vivo permeation studies; Vaginal mucosa; HIV-1.*

#### *Abbreviations*

*GBV* : GB virus C

*PLGA* : D, L-lactic-co-glycolic acid

*O.C.T* : Optimum cutting temperature

*PFA* : Paraformaldehyde

*E2-FAM*: E2 peptide labelled with 5(6)-carboxyfluorescein

*NPsE2-FAM*: Nanoparticles loaded with P6-2-FAM

#### 1. Introduction

The GB virus C (GBV-C) is a non-pathogenic member of Flaviviridae family; it is a lymphotropic virus that replicates in human peripheral blood mononuclear cells (PBMC), including B and T lymphocytes. [1]. Several studies show that: (a) GBV-C infection is associated with slower progression and prolonged survival in HIV-infected patients. (b) When GBV-C is added to CD4<sup>+</sup> T cells it inhibits HIV entry. (c) Transmission of HIV-1 from mother to child is reduced in mothers co-infected with GBV-C [2]. (d) The RNA<sup>+</sup> of GBV-C in HIV patients correlates with lower activation of T lymphocytes [3]. These findings have been used to develop new strategies against the spread of HIV.

Two GBV-C viral proteins, NS5A and E2, inhibit HIV replication *in vitro*. NS5A induces the expression of SDF-1 and down regulates CXCR4 in CD4<sup>+</sup> T cells. Moreover, NS5A may enhance the resistance of

CD4+ T cells to HIV infection [4]. The E2 envelope glycoprotein appears to inhibit the earlier steps of HIV infection, due to an internal fusion peptide that inhibits gp41 fusion to the cell targets [5]. The use of small peptides derived from GBV-C envelope proteins has thus been suggested as a strategy to inhibit HIV-infection [6–8].

In an attempt to decrease the rate of HIV infection, a broad range of HIV-1 fusion-entry inhibitors have been explored. Several HIV inhibitors have been reported to block the entry of HIV to target-cells. For example, VIRIP, a derivative from serine protease inhibitor ( $\alpha$ -1antitrypsine) inhibits HIV-1 entry by binding to the fusogenic peptide in gp41 (gp41-FP) and preventing its insertion into the target-cell [9]. Enfuvirtide (T-20), a peptide derived from gp41, blocks conformational changes in gp41 and thus inhibits HIV-1 fusion to cells [10]. E2, a peptide derived from the E2 envelope protein of GBV-C, interacts with the disulphide loop region in gp41 of HIV. E2 contains three cysteine residues, which may interfere with the oxidation state of the cysteine in the gp41 disulphide region. [11,12].

Unfortunately, peptides suffer from limitations such as: low oral bioavailability, short half-life, fast removal and poor ability to cross-physiological barriers. Moreover, hydrophobicity and flexibility can reduce specificity and trigger activation of different receptors or targets, leading to side effects [13].

HIV is mainly transmitted through infected vaginal and rectal mucosae. Research on the prevention of HIV infection has focused on the development of topical microbicides. However, the first-generation HIV microbicides failed as a result of genital epithelial disruption and inflammation [14]. Damage to the epithelial lining as a result of physical and chemical stress can increase the incidence of HIV, and facilitate penetration of submucosal tissue. Further, the microbiota change in the vaginal mucosa, following prolonged exposure to the high doses of drugs, could lead to a breakdown of the defense barrier in the mucosa and therefore facilitate HIV infection [15].

The vaginal fluid that covers the mucosa can help the microbicide to reach the epithelium, or remove the microbicide. Unless vaginal microbicides satisfy essential criteria of stability, safety, effectiveness and tolerability, their efficacy and toxicity might be compromised during permeation across mucosal tissue [16].

A new generation of HIV microbicides is being manufactured with biodegradable carriers such as liposomes, nanoparticles, dendrimers, gels, and films, in order to improve the safety and effectiveness of the drugs [16–18]. The systems most widely used for this purpose are nanoparticles made with polyesters such as poly (D, L-lactic-co-glycolic acid) (PLGA). This polymer has been approved by Food and Drug Administration (FDA) and used as colloidal carriers for drug controlled release [19]. It has several advantages such as biocompatibility, biodegradability and non-toxicity [20]. In addition, PLGA shows good reproducibility, controllable release and predictable degradation kinetics [21]. In addition, PLGA properties such as bioadherence and mucoadhesiveness are comparable to the mucoadhesive properties of biopolyaminosaccharides such as chitosan. Chitosan, a deacylated product of the linear polysaccharide chitin, has attracted attention as a potential absorption enhancer across mucosal epithelia [22–24].

Polymeric nanoparticles (NPs) have been considered as a suitable carrier to entrap proteins and polypeptides, since NPs target specific localization, which offers controllable and site-specific peptide release. In addition, NPs as carriers of anti-HIV peptides have the specific potential to address the main issues of traditional HIV-1 therapy, such as overcoming cellular and anatomical barriers, drug toxicity, drug resistance, suboptimal adherence and virus sequestration [25]. For example, NPs have been used extensively to entrap therapeutic peptides and to improve their activity. In this sense, an analogue of RANTES (PSC-RANTES) encapsulated in polymeric NPs maintained comparable anti-HIV activity with unformulated PSC-RANTES in HeLa cells. Studies *ex vivo* demonstrated that PSC-RANTES carried by NPs increased tissue uptake and enhanced both tissue permeation and leading localization at the basal layers of the epithelium compared with unformulated PSC-RANTES [26].

Here we developed PLGA Nanoparticles (NPs) covered with glycol-chitosan to encapsulate an HIV fusion inhibitor peptide (E2). Furthermore, we carried out assessments *ex vivo* and *in vivo* to examine the ability of NPs to reach the vaginal epithelium. The penetration rate was measured in a swine model using confocal microscopy.

## **2. Materials and methods**

### *2.1. Materials*

Fmoc-protected amino acids, NovaSyn TGA, TGR resins as well as 5(6)-carboxyfluorescein 5(6)-FAM were purchased from Novabiochem (Merck Millipore, Merck KGaA, Darmstadt, Germany). Peptide-synthesis-grade dimethylformamide (DMF) and trifluoroacetic acid (TFA) were obtained from Scharlau (Barcelona, Spain). Diethyl ether, dichloromethane (DCM) and methanol were obtained from Merck (KGaA, Darmstadt, Germany). 2-(1H-7-azabenzotriazole-1-yl)-1.1.3.3-tetramethyluronium hexafluorophosphate methanaminium (HATU) was from Genscript (Piscataway, NJ, USA). Diisopropylethylamine (DIPEA), piperidine, triisopropylsilane, N', N'-diisopropylcarbodiimide (DIPCDI), 1-hydroxybenzotriazole (HOBt), trimethylamine, Glycol Chitosan, 4-(2-Hydroxyethyl) piperazine-1-ethanesulfonic acid (HEPES); 1,4 dithiothreitol (DTT), Paraformaldehyde (PFA) were purchased from Fluka Sigma-Aldrich (St. Louis, MO, USA). PLGA 50:50 monomer ratio (RG 503H, mw 34 kDa,  $[\eta] = 0.32\text{--}0.44$ ) was purchased from Boehringer Ingelheim (Ingelheim, Germany). Polyvinyl alcohol (PVA) was obtained from BASF (Barcelona, Spain). Potassium dihydrogen phosphate, disodium hydrogen phosphate, acetic acid was from Panreac (AppliChem GmbH, Darmstadt, Germany) HPLC-grade acetonitrile (ACN) was purchased from Fisher Scientific (Loughborough, UK). Double-distilled water was obtained from a Milli-Q® Gradient A10 system apparatus (Millipore Iberia S: A: U; Madrid, Spain). Tissue-Tek® O.C.T. Compound was purchased from Sakura Finetek, USA. 1,5-bis {[2-(dimethylamine) ethyl] amino}-4,8-dihydroxyanthracene-9,10-dione (DRAQ5), were purchased from BD Biosciences, Transcutol®P was kindly donated by Gattefossé, (Madrid, Spain).

## 2.2 Methods

### 2.2.1 Synthesis of peptides

E2 peptide was synthesized by solid-phase peptide synthesis (SPPS) and Fmoc/*t*But. A NovaSyn TGA resin functionalized with hydroxymethylphenoxyacetic acid (HMPA) was acetylated with the symmetrical anhydride of the C-terminal amino acid (Fmoc-Gly-OH) as described by Gomara *et al.*, [27]. Couplings were performed by HATU/DIPEA activation with three-fold molar excess of Fmoc-amino acids. The Fmoc was deprotected twice with (20%) piperidine in DMF for 10 minutes. The stepwise addition of each residue was assessed by Kaiser's test and by the chloranil test for identification of secondary amines (proline residues).

Before the cleavage, the E2 peptidyl-resin was labelled at the N-terminus with 5(6)-carboxyfluorescein, 5(6)-FAM). The carboxylic acid group of the fluorescent dye was activated with N, N'-diisopropylcarbodiimide (DIPCDI) and hydroxybenzotriazole (HOBt). Coupling was carried out with three-fold molar excess of the reagents. Fluorescent labeling of the E2 peptidyl-resin was evaluated by Kaiser's test.

The peptide was side chain deprotected and cleaved from resins by a treatment of trifluoroacetic acid TFA, triisopropylsilane (TIS) and water: 9.5%, 2.5%, and 2.5. The reaction was carried out for 3 hours at room temperature. The solvents were evaporated in vacuum and the crude peptide was precipitated with cold diethyl ether. Precipitated peptide was dissolved in 30% glacial acetic acid in water and lyophilized. The peptide was purified by semi preparative HPLC (1260 Infinity, Agilent Technologies, Santa Clara, CA, USA) in an XBridge™ Prep C<sub>8</sub> column (5 μm, 10x 250 mm, Waters, Milford, MA, USA. E2 was analyzed using a Waters Alliance HPLC with diode array detector with analytical column Kromasyl 100 C18 column (250mm × 4.6mm, 5μm, Teknokroma). The analyses were carried out with linear gradient of 95% water (0.05% TFA) / 5% acetonitrile (0.05% TFA). The peptide was purified at 95% by analytical HPLC at 220 nm. E2 and E2-FAM were examined by electrospray ionization mass spectrometry (ESI-MS). The methods are reported in detail in supplementary materials section.

### 2.2.2. Preparation of the PLGA NPs loaded with E2-FAM (NPsE2-FAM)

The NPs were manufactured by a modified double emulsion method [28]. NPs with E2, E2-FAM and empty NPs were prepared individually. In brief, the NPs were prepared with 50 mg of PLGA dissolved in 1 mL of dichloromethane (organic phase). The preparation was then emulsified under sonication (30 s, 50 W) with a solution containing 1.5 mg of either E2 or E2-FAM, forming a water-in-oil-water emulsion (W<sub>1</sub>/O/W<sub>2</sub>). Afterwards, the first emulsion (W<sub>1</sub>/O) was added to 6 mL of previously prepared solution (2.5 % PVA and chitosan 0.05%, at pH 4.0) and the mixture was emulsified again by sonication (1 minute, 50W), forming a double emulsion (W<sub>1</sub>/O/W<sub>2</sub>). The emulsion was stirred overnight to evaporate the solvent and to form and harden the NPs.

NPs were purified by ultracentrifugation for 15 minutes, 15000 rpm; at 4°C (Beckman Coulter, OPTIMA L-100K), washed twice and suspended in Milli-Q water.

### 2.2.3. Physicochemical Characterization of the NPsE2

The average particle size ( $Z_{av}$ ) and polydispersity index (PI) of both NPsE2-FAM and NPsE2 were determined by photon correlation spectroscopy (PCS) (after 1:10 dilution) with a Zetasizer Nano ZS (Malvern Instruments, Malvern, UK) at 25 °C using disposable quartz cells and (Malvern Instruments).

NP surface charge, measured as Z Potential ( $\zeta$ ), was evaluated using laser-Doppler electrophoresis with M3 PALS system in ZetasizerNano ZS.  $\zeta$  indirectly indicates the rate of aggregation of particles. A greater  $\zeta$  (in absolute value) would induce less aggregation due to repulsion forces between the particles. The ZP was calculated applying the Henry equation [29].

$$\mu_E = \frac{\varepsilon \zeta f(Ka)}{6\pi\eta} \quad (1)$$

where  $\mu_E$  is the electrophoretic mobility,  $\varepsilon$  is the dielectric constant of the medium,  $\zeta$  is the zeta potential,  $\eta$  is the medium viscosity,  $Ka$  is the Debye-Hückel parameter and  $f(Ka)$  is a correction factor that considers the thickness of the electrical double layer ( $1/K$ ) and particle diameter represented by ( $a$ ). The unit of  $K$  is a reciprocal length. The reported values correspond to the mean  $\pm$  SD of at least three different batches of each formulation

### 2.2.4. Entrapment efficiency (EE %)

The EE percentage of the peptide loaded into the NPs was calculated indirectly by measuring the concentration of the peptide in the dispersion medium. The non-entrapped E2 was separated from the entrapped E2 by ultracentrifugation (at 15000 rpm for 15 minutes, 4°C). The concentration of the non-entrapped peptide was measured by HPLC UV-VIS. The HPLC system was connected to a Waters® 515 HPLC Pump (Waters, Milford, MA, USA). The analytical column was a Kromasil 100 C18 (250mm×4.6mm, 5 $\mu$ m, Teknokroma). The peptide was detected at 280 nm with a flow rate of 1.0 ml/min. The eluents were 95% water (0.05% TFA) and 5% acetonitrile (0.05% TFA) (95:5 v/v). Each sample was diluted with acetonitrile/ water (1:10). The EE (%) was determined applying Eq (2).

$$EE (\%) = \frac{\text{Total Amount of peptide} - \text{free peptide}}{\text{Total amount of peptide}} \cdot 100 \quad (2)$$

### 2.2.5. Amino acid analysis

The amino acids composing the peptide entrapped in the NPs were identified and quantified as described by Cohen *et al.*, [30,31]. In brief, 30  $\mu$ L of 1- amino-n-butyric acid (2.5 mM) and 1 mL of HCL 12 M were added to 1 mL of the sample (NPsE2 suspension, 166  $\mu$ g/mL of E2 peptide). Hydrolysis was carried out at 110 °C for 16 hours. The internal standard (10 mL) was added and diluted with water to 250 mL. The solution was passed through a 0.20  $\mu$ m filter. Then, the acid was evaporated and dried sample was dissolved with Milli-Q water.

Derivatization was performed by adding 70  $\mu$ L of borate buffer to 10  $\mu$ L of filtered hydrolysate sample or

standard. The optimal pH range for derivatization is 8.2–9.7, and the solution was briefly vortexed. Then, 20  $\mu\text{L}$  of reconstituted AccQ.Fluor reagent (3 mg/ml in acetonitrile) was added and the mixture was immediately vortexed. The vial was closed and left to stand for one minute at room temperature. It was then placed in a heating block at 50  $^{\circ}\text{C}$ , for 10 minutes.

Chromatographic separation was carried out in a Waters AccQ.Tag amino acid analysis Nova-Pak<sup>TM</sup> column (3.9 mm  $\times$  150 mm, 4  $\mu\text{m}$ ) fitted with a Nova-Pak<sup>TM</sup> C 18. The column was thermostatted at 37  $^{\circ}\text{C}$  and a flow rate of 1.0 mL/min. The injection volume was 20  $\mu\text{L}$ . Mobile phase A consisted of AccQ.Tag eluent A, (100 mL AccQ.Tag A concentrate + 1 L Milli-Q water). Mobile phases B and C were acetonitrile and Milli-Q water, respectively. Reaction of amino acids with 6-aminoquinolyl-N-hydroxysuccinimidyl carbamate yielded derivatives that were detected at 254 nm. Qualitative and quantitative analyses were based on retention times and internal standard method, respectively.

#### 2.2.6 Release studies in vitro

The evaluation of the peptide released from NPsE2 were carried out in amber glass Franz type diffusion cells (FDC-400) of 18 mm diameter. A dialysis cellulose membrane MW 12000-14000 Da (Iberoamerica, Spain) was hydrated with the receptor medium (pH 7.4 phosphate buffer 10 mM, DTT 10 mM) for 24 hours before use. The membrane was fastened between the donor and the receptor compartments of Franz cells. The donor compartment was filled with 1 mL of NPsE2. The receptor compartment was filled with 5 mL of the receptor medium. The available diffusion area was 0.62  $\text{cm}^2$ . The temperature of the assessment was controlled at 37  $\pm$  1 $^{\circ}\text{C}$  to mimic human body temperature. The sink conditions were sustained throughout the experiment for 10 hours. Aliquots of 100  $\mu\text{L}$  were withdrawn from the receptor chamber at fixed time intervals and immediately replaced with an equal volume of fresh buffer. The quantification of E2 released was analyzed by HPLC-MS/MS, using a validated method. The concentration of E2 released was measured as described previously for EE. The data are reported as the mean  $\pm$  SD of three replicates.

The amount of E2 released was adjusted to the Boltzmann Sigmoidal kinetic model (Samaha et al., 2009)[32].

$$m = \frac{A_1 - A_2}{1 + e^{(t-t_0)/k}} + A_2 \quad (4)$$

where ( $m$ ) is the mass of each sample expressed in ng. ( $A_1$ ) is the low  $Y$  limit, ( $A_2$ ) is the high  $Y$  limit, ( $k$ ) is the slope and ( $t_0$ ) represent the  $V_{50}$ .  $V_{50}$  is a modelistic parameter that can determine the time in which half of the maximum peptide is released. A nonlinear least-squares regression was performed using the WinNonLin software (WinNonLin professional edition version 3.3 and Graphpad prism version 6 Demo).

The methods used to detect and quantify E2 (HPLC MS/MS and HPLC UV-VIS), were validated following the ICH guidelines [33]. The HPLC UV-VIS method was validated using acetonitrile/water as the matrix, whilst the receptor medium was used to validate the HPLC MS/MS method. The parameters

studied were: linearity, by determination of slope, intercept, 95% confidence intervals and the regression coefficient ( $r$ ), limit of detection (LOD) and limit of quantification (LOQ). The precision inter-day was expressed as the mean of the coefficient of variation (CV). Accuracy was defined as the mean of the percentage deviation (EE) for the HPLC UV-VIS method, whilst the accuracy by HPLC MS/MS, was defined as the mean of recovery percentage (RE).

The validation parameters of HPLC UV-VIS and HPLC MS/MS are shown in Tables 2 and 5 respectively. The methods are reported in detail in supplementary materials section.

#### 2.2.7. Penetration of the NPsE2 in vaginal mucosa of swine

The penetration was evaluated using NPsE2 and NPsE2-FAM. NPs were carried out for both assessments *ex vivo* and *in vivo*. For assessments *ex vivo*, the vaginal mucosae were obtained from the animal house at Bellvitge (Barcelona University); according to protocol approved by Ethics Committee at the University of Barcelona. The mucosae were maintained in a cryoprotective solution and stored at -80 °C until use, following the protocol described by *Amores et al* [34].

##### 2.2.7.1. Evaluation *ex vivo* of the penetration rate of the NPsE2-FAM and the retained amount of E2

Both the penetration rate and the amount retained were measured using 5 mL Franz cells. The donor compartment contained either NPsE2 or NPsE2-FAM ( $n=3$ ), and the receptor compartment was filled with the mix of receptor medium and Transcutol P<sup>®</sup> 50:50 (v/v), so as to ensure a high solubility of E2. Diffusion testing was performed at 300 rpm and  $37 \pm 1$  °C. The full thickness mucosa discs were placed between the two cell compartments. The available diffusion area was 0.62 cm<sup>2</sup>. A clamp was used to hold the compartments together. Each assay was performed by triplicate.

To evaluate the penetration rate, at the end of the experiment (5 hours), the vaginal tissues were removed and fixed in paraformaldehyde 4% (PFA) for 24 hours. Subsequently, the tissues were immersed in sucrose 30% and embedded in the Tissue-Tek<sup>®</sup> O.C.T. compound, immersed in liquid nitrogen and stored at -80°C. 25 µm sections perpendicular to the mucosal surface were cut on a cryostat (Leica CM1510, Leica Microsystems) at -20 °C.

The cell nuclei of the tissues were stained with a solution of DRAQ5 (1:2000). The slides were observed using a confocal laser-scanning microscope (TCS-SL-Leica Microsystems) using  $\lambda_{exc}$ : 488 nm for the visualization of the NPsE2-FAM. The acquired images were processed by the means of IMAGE-J software.

To determine the retained E2 amount, at 5 hours intervals, aliquots of 300 µL were withdrawn from the receptor chamber and immediately replaced with an equal volume of receptor medium. At the end of the experiment, tissues were removed and rinsed in PBS and the permeation areas were cut and weighed. The E2 retained in the mucosa was extracted with a mixture of the receptor medium and acetonitrile (80:20, v/v); the solution and the mucosa were mixed for 20 minutes under cold sonication in an ultrasound bath. The E2 was quantified by HPLC/MS-MS and expressed as µg /g·cm<sup>2</sup>. The result was the average of three

independent experiments.

#### *2.2.7.2. Evaluation in vivo of the penetration rate of NPsE2-FAM*

Experiments were conducted using four female swine of 25 kg. Before carrying out the experiments, the animals were anesthetized. Aliquots of 1 mL of NPsE2-FAM (0.3 mg/mL) were poured, into the vaginal area. Afterwards, the animals were sacrificed by anesthesia overdose and intact vaginal mucosa was isolated using surgical scissors. Tissues slices were used to evaluate both the NP toxicity and the NPsE2-FAM penetration.

The penetration of NPsE2-FAM was analyzed using a confocal microscope. After the exposure (2 and 5 hours), the tissues were fixed by dipping them into PFA (4%) over-night, immersed in sucrose 30% for 5 hours, embedded in Tissue-Tek<sup>®</sup> O.C.T. compound and immersed in liquid nitrogen. 20  $\mu$ m sections perpendicular to the mucosa surface were cut on a cryostat (Leica CM1510, Leica Microsystems) at -20 °C. The nuclei were stained with DRAQ5. The slides were observed on a confocal laser-scanning microscope, using  $\lambda_{exc}$ : 488 nm for the visualization of NPsE2-FAM. The acquired images were processed by IMAGE-J software.

To evaluate the toxicity of NpsE2-FAM, water was applied to one untreated animal. This was to verify the normal tissue architecture and inflammation status in the vaginal mucosa, following the process mentioned above. Tissues were paraformaldehyde fixed, embedded in paraffin and stained with hematoxylin and eosin. Tissue slices were visually examined for histological features, in a blinded method, using a transmitted-light microscope (Epi-fluorescence microscopy, NIKON). The morphological condition of the vaginal mucosa was examined in 10 different slides.

#### *2.8. Statistical analyses*

Multiple comparisons were obtained by one-way ANOVA with either Turkey's or a run test, except the histological and confocal studies, which were acquired by using a specific program (Image J). Data are presented as a mean  $\pm$  SD

### *3. Results and discussion*

#### *3.1. Peptide synthesis*

E2 is a 20-mer peptide [LCDCPNGPWVWVPAFCQAVG], with a MW of 2165, characterized by its high hydrophobic content and the presence of three cysteine residues [11]. These properties enable it to interact with the sequence in the disulphide-loop region in gp41 and to block HIV-1 fusion to the cells. Their specificity and activity was confirmed by comparison with a peptide in which the amino acids were arranged randomly (random peptide). The random peptide showed significantly higher IC<sub>50</sub> values against two different HIV strains than the parent sequence. These findings confirmed that E2 may interfere with the fusion and entry of the HIV-1 to the host cell [12]. In the present study, the peptide and its fluorescent derivative (E2-FAM) were successfully synthesized to a high degree of purity (>95%) after HPLC semi

preparative purification.

### 3.2. Characterization of NPs

The aim of the study was to examine whether NPs could cross the first defense barrier on the surface of the mucosa and reach the epithelium without harming the epithelial lining. Our work also involved preparing PLGA NPs covered with glycol chitosan (GC) to entrap an HIV-1 inhibitor peptide and then release it into the vaginal mucosa of the swine. Chitosan is a natural polysaccharide composed of D-glucosamine and N-acetyl D-glucosamine units. GC is the chitosan conjugated with ethylene glycol, it is water soluble below pH 5.0 and, at the same time, it retains its positive charge at physiological pH values [35]. The properties of the NPs obtained are summarized in Table 1. The formulation shows an average size ( $Z_{av}$ ) of roughly 304 nm, PI values of 0.180;  $\zeta$  of  $30.6 \text{ mV} \pm 4.2$  and suitable entrapment efficiency. Previous studies have reported that NPs with diameters around 200-500 nm can permeate faster through the vaginal mucus [16]. Therefore, the presence of chitosan may increase the mucoadhesiveness of NPs and the retention time at the administration site, providing them with a positive superficial charge. In addition, chitosan has been associated with the improvement of peptide transport across the epithelial barrier [36].

Table 1. Physicochemical properties and EE of NPs<sub>E2</sub> and NPs<sub>E2</sub>-FAM

Formulations	$Z_{av} \pm SD$ (nm)	PI $\pm DS$	$\zeta \pm SD$ (mV)	EE $\pm SD$ (%)
NPs <sub>E2</sub> <sup>(a)</sup>	$305.30 \pm 3.13$	$0.180 \pm 0.014$	$30.6 \pm 0.35$	$62.01 \pm 1.89$
NPs <sub>E2</sub> -FAM <sup>(a)</sup>	$326.10 \pm 6.99$	$0.210 \pm 0.007$	$32.5 \pm 1.31$	$66.67 \pm 2.81$

Notes: Values are average of three independent batches, and are expressed as mean SD

Abbreviations:  $Z_{av}$ , average size; EE, entrapment efficiency; NPs, Nanoparticles; PI, polydispersity index;  $\zeta$ , Zeta potential and SD, standard deviation

Table 2. Validation of E2 detection by HPLC UV-VIS method

Range ( $\mu\text{g/ml}$ )	Slope	Intercept	Regression coefficient	LOD ( $\mu\text{g/ml}$ )	LOQ $\mu\text{g/ml}$	<sup>(a)</sup> Accuracy Recovery (%)	<sup>(b)</sup> Precision C.V (%)
27.5 – 220.0	6141	-14418	1	$6.8 \pm 4.3$	$20.6 \pm 11.73$	$100.17 \pm 0.84$	$\pm 4.8$

<sup>(a)</sup>. The accuracy is expressed as overall recovery percentage (n=5).

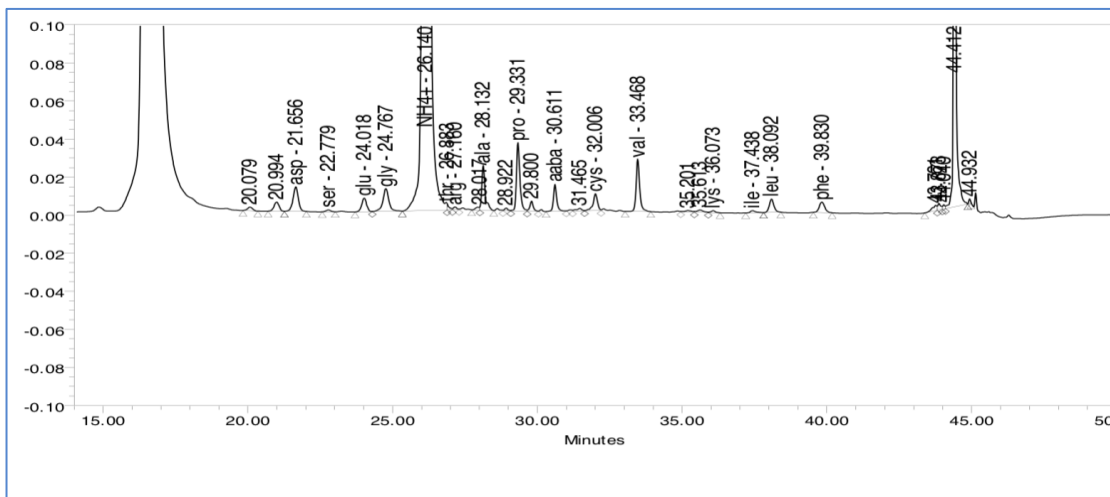
<sup>(b)</sup>Precision intraday was obtained by back-calculated concentration for each calibration curve (n=5).

Acceptance criterion  $\pm 10\%$

#### 3.2.1. Amino acid analysis

Chromatograms corresponding to amino acids from the NPs<sub>E2</sub>, obtained after acid hydrolysis, are shown in Figure 1. The amino acids content of the analyzed NPs<sub>E2</sub> suspension are reported in Table 3. Asparagine and glutamine were deamidated to their respective acids during hydrolysis. They are reported

together as Asp/Asn and Glu/Gln. Tryptophan was destroyed during HCl hydrolysis. Proline, glycine and valine were the most abundant amino acids in the sample. The amino acid content in the sample was 0.055 mM (109  $\mu$ mL), which corresponding to 66.65% of total peptide added to NPs. This result is consistent with the results obtained by HPLC UV-VIS method at 280 nm (62.01 %).



Peak name	RT	Area	% Area	Height	Amount
Asp	21.656	164441	12983	12983	0.095
Ser	22.779	10477	914	914	0.005
Glu	24.018	85951	7155	7155	0.051
Gly	24.767	171911	12043	12043	0.100
Hys	25.267				
NH <sub>4</sub> <sup>+</sup>	26.140	11490029	67.85	888515	
Thr	26.883	14995	0.09	3306	0.007
Arg	27.160	11346	0.07	1389	0.006
	28.017	14242	0.08	1565	
Ala	28.132	190431	1.12	23484	0.094
	28.992	10982	0.06	1370	
Pro	29.331	297451	1.76	35863	0.159
	29.800	44513	0.26	5303	
Aaba	30.611	115525	0.68	14325	0.071
	31.465	18048	0.11	1408	
Cys	32.006	96253	0.57	8884	0.064
Tyr	32.540				
Val	33.468	238993	1.41	27570	0.128
Met	34.028				
	35.201	13795	0.08	820	
	35.613	18033	0.11	1202	
Lys	36.073	10921	0.06	1022	0.004
Ile	37.438	14404	0.09	1126	0.007
Ileu	38.092	77026	0.45	6921	0.040
Nle	38.967				
Phe	39.830	72397	0.43	5486	0.042
Trp	41.604				

**Figure 1.** Chromatogram corresponding to the amino acid analyses of NPsE2

Table 3. Amino acids contents in the NPsE2 suspension analysed

	<b>Amino acids</b>	<b>nmol</b>	<b>Theoretical</b>	<b>Report</b>
<b>2</b>	Asp/Asn	1.668	<b>2</b>	1.61
<b>3</b>	Thr	0.052	<b>0</b>	0.05
<b>5</b>	Glu/Gln	0.983	<b>1</b>	* 0.95
<b>6</b>	Pro	3.375	<b>3</b>	* 3.25
<b>7</b>	Gly	2.172	<b>2</b>	* 2.09
<b>8</b>	Ala	2.172	<b>2</b>	* 2.09
<b>9</b>	Cys	1.371	<b>3</b>	1.32
<b>10</b>	Val	2.767	<b>3</b>	* 2.67
<b>11</b>	Met	0.065	<b>0</b>	0.06
<b>12</b>	Ile	0.091	<b>0</b>	0.09
<b>13</b>	Leu	0.944	<b>1</b>	* 0.91
<b>14</b>	Tyr	0.065	<b>0</b>	0.06
<b>15</b>	Phe	1.073	<b>1</b>	* 1.03
<b>16</b>	His	0.181	<b>0</b>	0.17
<b>17</b>	Lys	0.078	<b>0</b>	0.08
<b>19</b>	Arg	0.168	<b>0</b>	0.16

The amino acids that were used for calculations are those marked an asterisk (\*).

### 3.2.2. Release in vitro

Figure 2 shows a bi-phasic release profile of E2, characterized by an induction phase (phase I), followed by a sustained phase (phase II). The asymptote was reached at 5 hours, maintaining a lag-phase up to 10 hours. The release studies were performed for 24 hours, but after 10 hours, the peptide detection was imprecise. This finding was attributed to peptide aggregation in the medium and adsorptive problems. Thus, DTT was added in the release medium to prevent the aggregation, and the time of the assays was also limited to 10 hours. During this period, the peptide was easier to detect by HPLC/MS-MS. Although not all the peptide incorporated into NPs was released, the results were fitted to the Boltzmann sigmoidal model. Table 4 shows the model and the corresponding dissolution parameters for statistical analysis of E2 released from NPs.

A recent study reported that E2 release from liposomes was slower in buffer (PBS) than in a culture medium supplemented with 10% fetal bovine serum DMEM/FBS[27]. Although the release mechanisms of polymer systems are different from those of liposomes, similar results were obtained in the present study: approximately 10% of the peptide encapsulated in NPs was released in the PBS receptor medium. This suggests that the E2 release profile was slowed down, either as a result of a dense polymer with low porosity, or due to peptide-polymer interactions

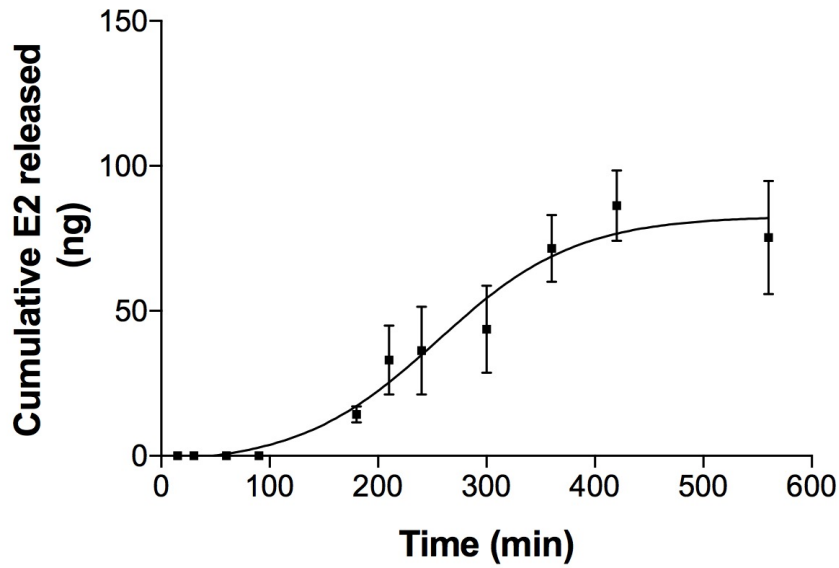


**Figure 2.** Cumulative *in vitro* release profile of E2 entrapped in PLGA NPs covered with GC. Data shown are average values from experiments performed in triplicate

Table 4. Release kinetic parameters for free E2 in solution and E2 entrapped in PLGA Nanoparticles

	Bottom (µg)	Top (µg)	V50	Slope	$r^2$
NPsE2	$-3.15 \pm 5.64$	$82.60 \pm 6.87$	$254.600 \pm 18.40$	$63.64 \pm 19.15$	0.989

### 3.3. Evaluation *ex vivo* the penetration of NPsE2-FAM and the amount of the E2 retained

To evaluate the transit of the NPs loaded with E2-FAM to the vaginal epithelium, assays with cryopreserved mucosae were conducted *ex vivo* using the Franz Cells systems. To our knowledge, no study has reported that NPsE2 penetrates vaginal mucosa. However, some authors have described the use of NPs as carriers of antiretroviral drugs. For example, Das Neves and co-workers [16], reported that polymeric NPs measuring about 200 nm loaded with Dapivirine penetrated the excised vaginal mucosa of swine. In the present study, the NPsE2-FAM of 300 nm also penetrated the vaginal mucosa. The NPsE2-FAM penetration was evaluated by confocal microscopy and the images show a fluorescent signal at the upper-layer of the epithelium attributed to the NPsE2-FAM (Figure 3a). These observations suggest that the adhesion of the NPsE2-FAM to the epithelium is due to the mucoadhesivity and bioadherence features associated with such systems. Some fluorescent aggregates were also found in the deep zones of the mucosa. The peptide released from NPs and/or NPsE2-FAM may pass through the epithelium by passive diffusion. Lipophilic molecules, such as E2, may cross the epithelial cell layers by the intercellular route or diffusion. The intercellular route may pass through the lipid bilayers or along the narrow aqueous regions associated with polar head groups of the membrane lipids. If so, the peptide

would hinder the entry of HIV-1 to the intercellular space, thus preventing fusion of the virus to target cells.

Besides assessing the NPsE2-FAM penetration, the amount ( $Q_r$ ), of E2 retained was also measured, and found to be  $26.66 \pm 7.23 \text{ ng/g}\cdot\text{cm}^2$  ( $n=3$ ),  $p<0.05$ . The E2 permeation flux through the vaginal tissue was not calculated, as it was only detected after 5 hours of the experiment. The amount of E2 permeated at 5 hours was  $2.07 \pm 0.65 \text{ ng/cm}^2$  ( $n=3$ ),  $p<0.05$ . The amount of E2 permeating through the swine's vagina was lower than that retained in the tissue. This pattern might be repeated within the human mucosa. If the peptide levels in the mucosa were higher than the E2 systemic levels, the chances of blocking the HIV fusion to target-cells would increase and the viral resistance would decrease, which would reduce the adverse effects. The results suggest that diffusion and retention of the NPs/peptide may be influenced by its size and by the pathway through which the peptide crosses the mucosa.

Table 5. Validation of E2 detection by HPLC MS/MS method

Range (ng/mL)	Slope	Intercept	Regression coefficient	LOD ng/mL	LOQ ng/mL	<sup>(a)</sup> Accuracy RE (%)	<sup>(b)</sup> Precision CV (%)
1 - 100	1149	4147	0.9984	$1.93 \pm 0.96$	$5.86 \pm 2.92$	$\pm 9.6$	$\pm 8.87$

<sup>(a)</sup>Accuracy was evaluated by calculating residual values from linear regression of four calibration curves ( $n=4$ ).

<sup>(b)</sup>Precision intraday was obtained by back calculated concentration for each calibration curve ( $n=4$ ). Acceptance criterion  $\pm 10\%$

### 3.4. Evaluation in vivo of penetration of the NPsE2-FAM

In contrast to other studies *in vivo*, in which mice were used to examine the transit of nanoparticles across the vaginal mucosa [37], our we studied swine vaginal mucosa, which is considered to be similar to human tissue [38]. In addition, both consist of a stratified squamous epithelium supported by connective tissue and of the lamina propria, and they have a similar lipid composition, which is an important aspect of the defense barrier [39].

The NPsE2-FAM were instilled along vaginal area. At 2 hours and 5 hours post-treatment the animals were sacrificed by anesthesia overdose and the vaginas were extracted. At 2 hours post-treatment, the fluorescent signal was distributed over the surface vaginal epithelial layer (Fig.3 b and c). This indicates that the NPs migrate across the mucus reaching the epithelium and spreading within the adjacent epithelial layers. However, at 5 hours post-treatment, the penetration profile had changed. The fluorescence signal was distributed only in the first epithelial layer (plane cells) with lowest signal intensity. At 5 hours, the NPs/Peptide may have diffused through the tissue. If peptide is released, it may penetrate the mucosa through lipid bilayers and interact with cellular membranes, increasing their concentration near the fusion sites within intercellular space. In the absence of the virus, the peptide might be degraded by enzymes present in the mucosa or removed by systemic withdrawal. Furthermore, in all the slides a high concentration of NPs/peptide was observed inside a certain type of cells, which

implies that some cells may take up the NPs/peptide. Future studies will examine this hypothesis.

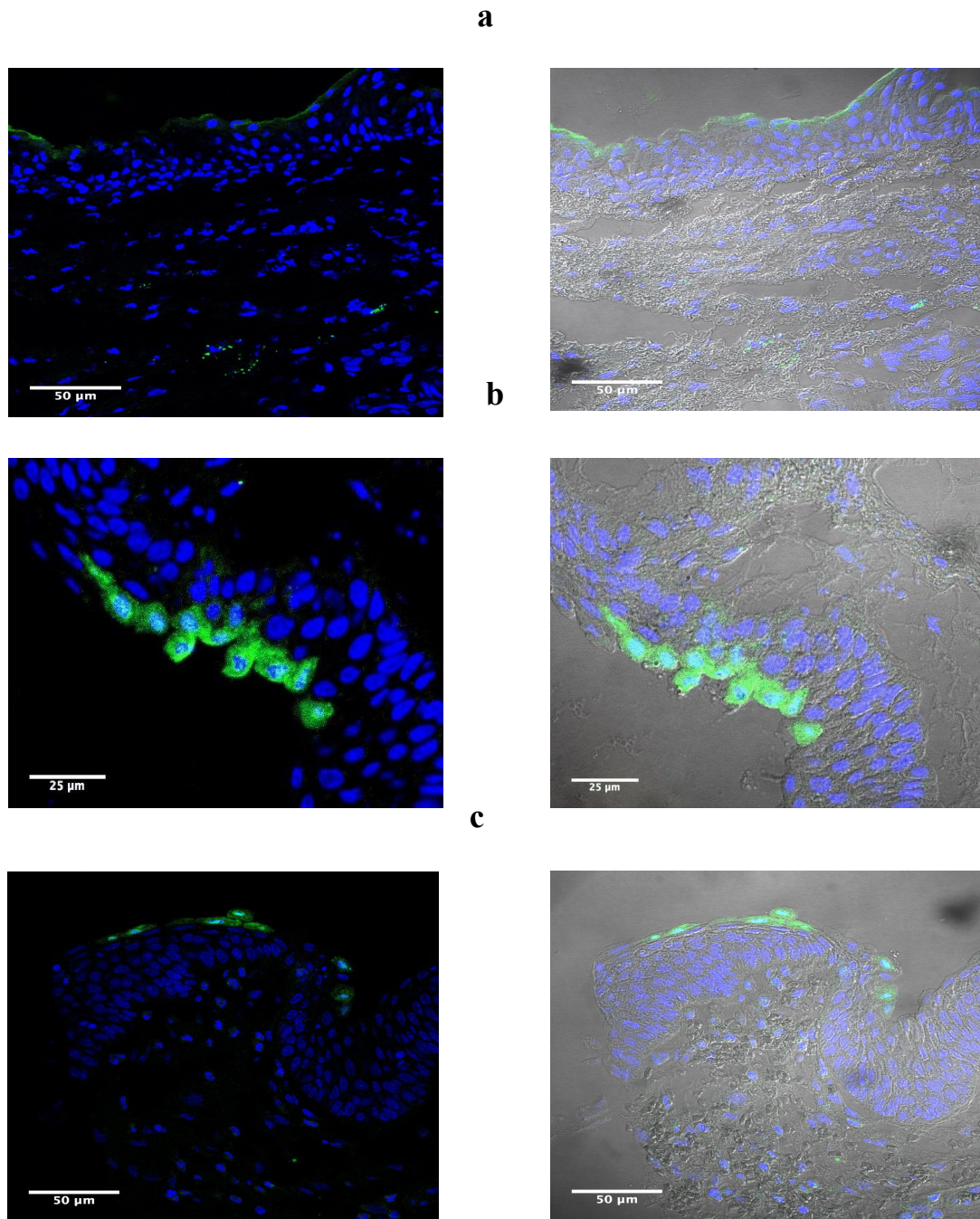


**Figure 3.** Confocal images of the vaginal epithelium of swine were acquired after treatment with NPsE2-FAM (transverse slices). The NPsE2-FAM were localized at the upper-layer of the vaginal epithelium (green). The nuclei were stained with DRAQ5 (blue). Fluorescence images (*left column*) and their respective differential interference contrast (DIC) images (*right column*) were acquired at 63X. **(a)** *Ex vivo* penetration rate, (5 hours). **(b)** *In vivo* penetration rate, (2 hours). **(c)** *In vivo* penetration rate, (5 hours).

### 3.5 Toxicity after application of the NPsE2-FAM in vivo

Several methods have been used to explore the safety of anti-HIV microbicides. Many of them are cell-based assays *in vitro*; these establish the cytotoxic concentration of the drug, CC50, which is the concentration that reduces cell viability by 50 %, and the maximum effective concentration, EC50, which is the concentration that gives half-maximal response. These are essential parameters when developing formulations with suitable doses. However, these assays do not allow us to assess the tissue damage, such as the detachment of the epithelium as a result of drug-induced toxicity or the inflammatory effects of prolonged exposure. Histologic analyses are widely used to evaluate the toxicity after vaginal application of microbicides. The loss of the structure and the presence of inflammatory infiltrates in the lamina propria have been considered an important cytotoxicity issue related to sustained exposure to drugs [40,41].

To determine harm, inflammation or epithelial upper-layer detachment, caused by NPsE2 or its degradation products, several slices of mucosa were cut and evaluated by microscopy. The number of epithelial layers in untreated mucosae was compared with the number of epithelial layers in the mucosa treated with NPsE2. In all the slices observed, the number of epithelial layers post-administration was the same as the number of epithelial layers on the untreated mucosa (n=10). There was no evidence of histopathological abnormality; leukocyte infiltration to the lamina propria or epithelial lesions related to the treatment with NPsE2-FAM. Figure 4 (a to c) shows a conserved mucosa with a multi-layer epithelium followed by connective tissue. This parameter is an indication of the safety of the NPs administered to vaginal mucosa

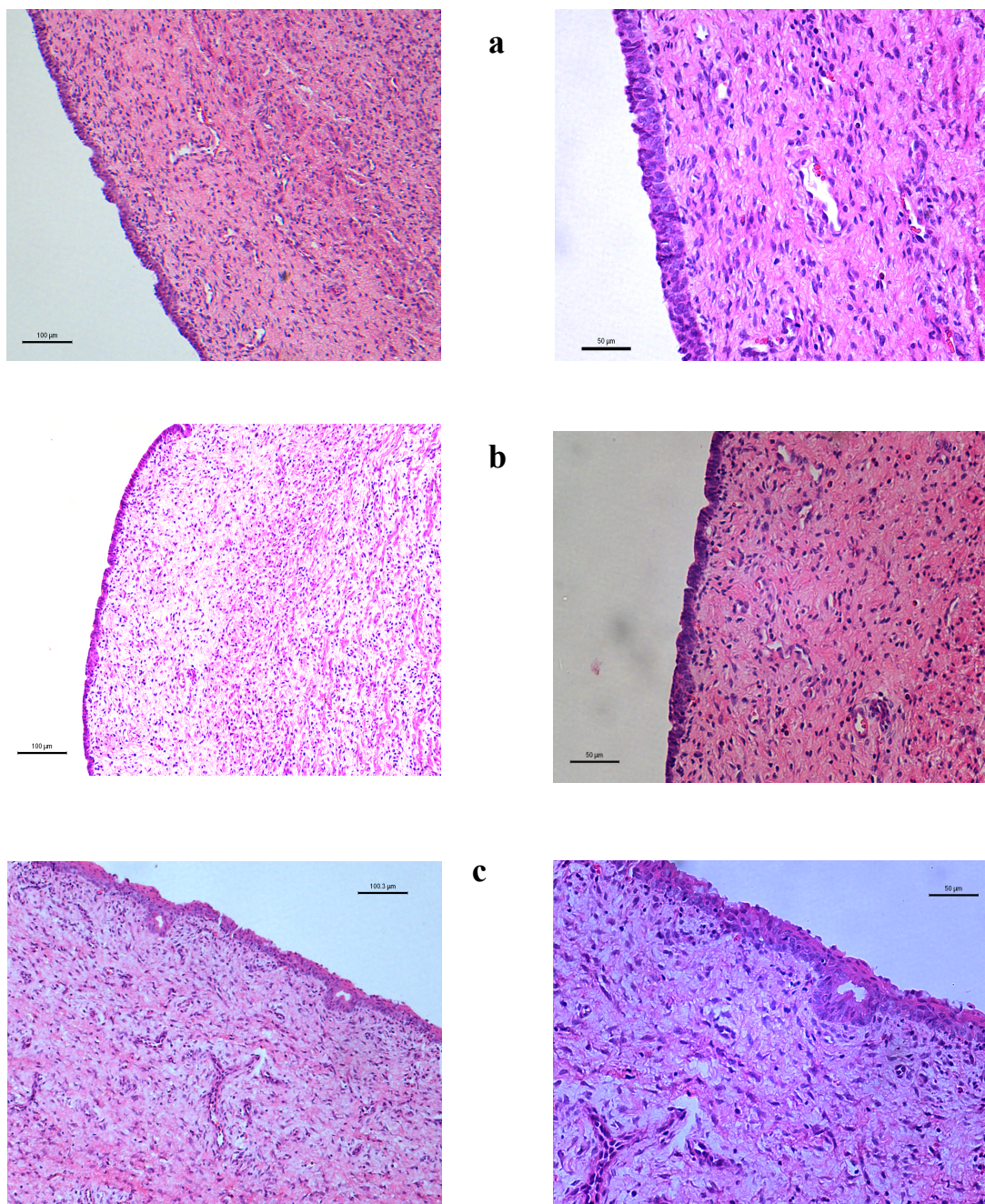


**Figure 4.** Histopathological images were acquired at 100X, (*left column*) and 10X (*right column*), (transverse slices). (a) Vaginal epithelium not exposed to NPSE2-FAM (*control*), (b) Vaginal epithelium after 2 hours of treatment with NPSE2-FAM, (c) Vaginal epithelium after 5 hours of treatment with NPSE2-FAM.

#### *4. Conclusions*

We present novel polymeric NPs covered with glycol-chitosan, which were successfully used to incorporate an HIV-1 inhibitor peptide, derived from GB virus C. NPsE2 has interesting physicochemical and morphological features that provide it with mobility across the mucus, to reach the vaginal epithelium and release the peptide. Besides, the localization of the NPsE2-FAM at the upper-layers of the epithelial mucosa was considered a key aspect, since the peptide may be released at the site where HIV transmission occurs. Overall data indicate that NPsE2 is an interesting approach for the development of putative anti-HIV microbicides

#### **Acknowledgment**

The authors thank the study participants Dr. Joan Blasi for the valuable insights throughout the manuscript development and Dr. Alvaro Gimeno for his advice and assistance with the animal experimental procedures. This research was supported by grants from the Spanish Ministry of Economy and Competitiveness (MAT2014-59134R and CTQ2015-63919R).

**Appendix A. Supplementary section.** An online version of the supplementary section associated with this article can be found at:

## REFERENCES

- [1] J.C. Arroyave, F.H. Pujol, M.C. Navas, F.M. Cortés-Mancera, [Interaction between HIV-1 and GB virus type-C during coinfection status], *Rev. Chilena Infectol.* 30 (2013) 31–41. doi:10.4067/S0716-10182013000100005.
- [2] W.B. Supapol, R.S. Remis, J. Raboud, M. Millson, J. Tappero, R. Kaul, P. Kulkarni, M.S. McConnell, P.A. Mock, M. Culnane, J. Menicholl, A. Roongpisuthipong, T. Chotpitayasunondh, N. Shaffer, S. Butera, Reduced Mother-to-Child Transmission of HIV Associated with Infant but not Maternal GB Virus C Infection, *J. Infect. Dis.* 197 (2008) 1369–1377. doi:10.1086/587488.
- [3] M.T. Maidana Giret, E.G. Kallas, GBV-C: State of the art and future prospects, *Curr HIV/AIDS Rep.* 9 (2012) 26–33. doi:10.1007/s11904-011-0109-1.
- [4] J. Xiang, J.H. McLinden, Q. Chang, T.M. Kaufman, J.T. Stapleton, An 85-aa segment of the GB virus type C NS5A phosphoprotein inhibits HIV-1 replication in CD4<sup>+</sup> Jurkat T cells, *Proc. Natl. Acad. Sci.* (2006) 1–6.
- [5] E.L. Mohr, J.T. Stapleton, GB virus type C interactions with HIV: the role of envelope glycoproteins, *J. Viral Hepat.* 16 (2009) 757–768. doi:10.1111/j.1365-2893.2009.01194.x.
- [6] L. Fernández, W.C. Chan, M. Egido, M.J. Gómara, I. Haro, Synthetic peptides derived from an N-terminal domain of the E2 protein of GB virus C in the study of GBV-C/HIV-1 co-infection, *J. Pept. Sci.* 18 (2012) 326–335. doi:10.1002/psc.2403.
- [7] M.J. Sánchez-Martín, K. Hristova, M. Pujol, M.J. Gómara, I. Haro, M. Asunción Alsina, M. Antònia Busquets, Analysis of HIV-1 fusion peptide inhibition by synthetic peptides from E1 protein of GB virus C, *J. Colloid Interface Sci.* 360 (2011) 124–131. doi:10.1016/j.jcis.2011.04.053.
- [8] M.J. Gómara, V. Sánchez-Merino, A. Paús, A. Merino-Mansilla, J.M. Gatell, E. Yuste, I. Haro, Definition of an 18-mer Synthetic Peptide Derived from the GB virus C E1 Protein as a New HIV-1 Entry Inhibitor, *Biochim. Biophys. Acta - Gen. Subj.* 1860 (2016) 1139–1148. doi:10.1016/j.bbagen.2016.02.008.
- [9] J. Münch, L. Ständker, K. Adermann, A. Schulz, M. Schindler, R. Chinnadurai, S. Pöhlmann, C. Chaipan, T. Biet, T. Peters, B. Meyer, D. Wilhelm, H. Lu, W. Jing, S. Jiang, W.G. Forssmann, F. Kirchhoff, Discovery and Optimization of a Natural HIV-1 Entry Inhibitor Targeting the gp41 Fusion Peptide, *Cell.* 129 (2007) 263–275. doi:10.1016/j.cell.2007.02.042.
- [10] J.M. Kilby, S. Hopkins, T.M. Venetta, B. DiMassimo, G.A. Cloud, J.Y. Lee, L. Alldredge, E. Hunter, D. Lambert, D. Bolognesi, T. Matthews, M.R. Johnson, M.A. Nowak, G.M. Shaw, M.S. Saag, Potent suppression of HIV-1 replication in humans by T-20, a peptide inhibitor of gp41

mediated virus entry., *Nat. Med.* 4 (1998) 1302–7. doi:10.1038/3293.

- [11] K. Eissmann, S. Mueller, H. Sticht, S. Jung, P. Zou, S. Jiang, A. Gross, J. Eichler, B. Fleckenstein, H. Reil, HIV-1 fusion is blocked through binding of GB Virus C E2-derived peptides to the HIV-1 gp41 disulfide loop [corrected]., *PLoS One.* 8 (2013) e54452. doi:10.1371/journal.pone.0054452.
- [12] Y. Koedel, K. Eissmann, H. Wend, B. Fleckenstein, H. Reil, Peptides derived from a distinct region of GB virus C glycoprotein E2 mediate strain-specific HIV-1 entry inhibition., *J. Virol.* 85 (2011) 7037–7047. doi:10.1128/JVI.02366-10.
- [13] P. Vlieghe, V. Lisowski, J. Martinez, M. Khrestchatisky, Synthetic therapeutic peptides : science and market, *Drug Discov. Today.* 15 (2010). doi:10.1016/j.drudis.2009.10.009.
- [14] V. Halpern, F. Ogunsoola, O. Obunge, C.H. Wang, N. Onyejebu, O. Oduyebo, D. Taylor, L. McNeil, N. Mehta, J. Umo-Otong, S. Otusanya, T. Crucitti, S. Abdellati, Effectiveness of cellulose sulfate vaginal gel for the prevention of HIV infection: Results of a phase III trial in Nigeria, *PLoS One.* 3 (2008) 1–8. doi:10.1371/journal.pone.0003784.
- [15] Y. Wang, K. Hida, R. Cone, M. Sanson, Y. Vengrenyuk, J. Liu, K. Moore, M. Garabedian, A. Edward, Correction for Lai et al., Nanoparticles reveal that human cervicovaginal mucus is riddled with pores larger than viruses, *Proc. Natl. Acad. Sci.* 108 (2011) 14371–14371. doi:10.1073/pnas.1111693108.
- [16] J. Das Neves, F. Araújo, F. Andrade, J. Michiels, K.K. Ariën, G. Vanham, M. Amiji, M.F. Bahia, B. Sarmiento, In vitro and Ex Vivo evaluation of polymeric nanoparticles for vaginal and rectal delivery of the anti-HIV drug dapivirine, *Mol. Pharm.* 10 (2013) 2793–2807. doi:10.1021/mp4002365.
- [17] Y. Gao, A. Yuan, O. Chuchuen, A. Ham, K.H. Yang, D.F. Katz, Vaginal deployment and tenofovir delivery by microbicide gels, *Drug Deliv. Transl. Res.* 5 (2015) 279–294. doi:10.1007/s13346-015-0227-1.
- [18] B. Pradines, C. Bories, C. Vauthier, G. Ponchel, P.M. Loiseau, K. Bouchemal, Drug-free chitosan coated poly(isobutylcyanoacrylate) nanoparticles are active against *Trichomonas vaginalis* and non-toxic towards pig vaginal mucosa, *Pharm. Res.* 32 (2015) 1229–1236. doi:10.1007/s11095-014-1528-7.
- [19] J.M. Anderson, M.S. Shive, Biodegradation and biocompatibility of PLA and PLGA microspheres, *Adv. Drug Deliv. Rev.* 64 (2012) 72–82. doi:10.1016/j.addr.2012.09.004.
- [20] S.A. Salem, N.M. Hwei, A. Bin Saim, C.C.K. Ho, I. Sagap, R. Singh, M.R. Yusof, Z. Md Zainuddin, R. Bt. Hj Idrus, Polylactic-co-glycolic acid mesh coated with fibrin or collagen and

- biological adhesive substance as a prefabricated, degradable, biocompatible, and functional scaffold for regeneration of the urinary bladder wall, *J. Biomed. Mater. Res. - Part A*. 101 A (2013) 2237–2247. doi:10.1002/jbm.a.34518.
- [21] N. Graf, D.R. Bielenberg, N. Kolishetti, C. Muus, J. Banyard, O.C. Farokhzad, S.J. Lippard, alpha V beta 3 Integrin-Targeted PLGA-PEG Nanoparticles for Enhanced Anti-tumor Efficacy of a Pt (IV) Prodrug, *ACS Nano*. 6 (2012) 4530–4539. doi:10.1021/nn301148e.
- [22] M.C. Bonferoni, G. Sandri, S. Rossi, F. Ferrari, S. Gibin, C. Caramella, Chitosan citrate as multifunctional polymer for vaginal delivery. Evaluation of penetration enhancement and peptidase inhibition properties, *Eur. J. Pharm. Sci.* 33 (2008) 166–176. doi:10.1016/j.ejps.2007.11.004.
- [23] Y. Tao, H.L. Zhang, Y.M. Hu, S. Wan, Z.Q. Su, Preparation of chitosan and water-soluble chitosan microspheres via spray-drying method to lower blood lipids in rats fed with high-fat diets, *Int. J. Mol. Sci.* 14 (2013) 4174–4184. doi:10.3390/ijms14024174.
- [24] A.S. Narang, S.H. Boddu, *Excipient Applications in Formulation Design and Drug Delivery*, Springer International Publishing Switzerland, 2015.
- [25] R. Parboosing, G.E.M. Maguire, P. Govender, H.G. Kruger, Nanotechnology and the treatment of HIV infection, *Viruses*. 4 (2012) 488–520. doi:10.3390/v4040488.
- [26] Anthony S. Ham, M.R. Cost, A.B. Sassi, C.S. Dezzutti, L.C. Rohan, Targeted Delivery of PSC-RANTES for HIV-1 Prevention using Biodegradable Nanoparticles, *Pharm. Res.* 26 (2014) 502–511. doi:10.1007/s11095-008-9765-2.Targeted.
- [27] M.J. Gómara, I. Pérez-Pomeda, J.M. Gatell, V. Sánchez-Merino, E. Yuste, I. Haro, Lipid raft-like liposomes used for targeted delivery of a chimeric entry-inhibitor peptide with anti-HIV-1 activity, *Nanomedicine Nanotechnology, Biol. Med.* (2016) 1–9. doi:10.1016/j.nano.2016.08.023.
- [28] F.T. Meng, G.H. Ma, W. Qiu, Z.G. Su, W/O/W double emulsion technique using ethyl acetate as organic solvent: Effects of its diffusion rate on the characteristics of microparticles, *J. Control. Release*. 91 (2003) 407–416. doi:10.1016/S0168-3659(03)00273-6.
- [29] E. Vega, F. Gamisans, M.L. García, A. Chauvet, F. Lacoulonche, M.A. Egea, PLGA nanospheres for the ocular delivery of flurbiprofen: Drug release and interactions, *J. Pharm. Sci.* 97 (2008) 5306–5317. doi:10.1002/jps.21383.
- [30] S.A. Cohen, K.M. De Antonis, Applications of amino acid derivatization with 6-aminoquinolyl-N-hydroxysuccinimidyl carbamate. Analysis of feed grains, intravenous solutions and glycoproteins, *J. Chromatogr. A*. 661 (1994) 25–34. doi:10.1016/0021-9673(93)E0821-B.
- [31] S.A. Cohen, D.P. Michaud, Synthesis of a fluorescent derivatizing reagent, 6-aminoquinolyl-N-

- hydroxysuccinimidyl carbamate, and its application for the analysis of hydrolysate amino acids via high-performance liquid chromatography., *Anal. Biochem.* 211 (1993) 279–287. doi:10.1006/abio.1993.1270.
- [32] D. Samaha, R. Shehayeb, S. Kyriacos, Modeling and comparison of dissolution profiles of diltiazem modified-release formulations, *Dissolution Technol.* 16 (2009) 41–46.
- [33] V. of A.P. and M.Q. (ICH), International Conference on Harmonisation, (ICH)Harmonised Tripart. Guidel. step 4 (2005).
- [34] E. Muthu, P. Balakrishnan, R. Vignesh, V. Velu, P. Jayakumar, S. Solomon, Current Views on the Pathophysiology of GB Virus C Coinfection with HIV-1 Infection, *Curr Infect Dis Rep.* 13 (2011) 47–52. doi:10.1016/j.ejps.2014.04.017.
- [35] A. Trapani, J. Sitterberg, U. Bakowsky, T. Kissel, The potential of glycol chitosan nanoparticles as carrier for low water soluble drugs, *Int. J. Pharm.* 375 (2009) 97–106. doi:10.1016/j.ijpharm.2009.03.041.
- [36] S.M. Van Der Merwe, J.C. Verhoef, J.H.M. Verheijden, A.F. Kotzé, H.E. Junginger, Trimethylated chitosan as polymeric absorption enhancer for improved peroral delivery of peptide drugs, *Eur. J. Pharm. Biopharm.* 58 (2004) 225–235. doi:10.1016/j.ejpb.2004.03.023.
- [37] C. Cunha-Reis, A. Machado, L. Barreiros, F. Araújo, R. Nunes, V. Seabra, D. Ferreira, M.A. Segundo, B. Sarmiento, J. das Neves, Nanoparticles-in-film for the combined vaginal delivery of anti-HIV microbicide drugs, *J. Control. Release.* 243 (2016) 43–53. doi:10.1016/j.jconrel.2016.09.020.
- [38] A.D. Van Eyk, P. Van Der Bijl, Porcine vaginal mucosa as an in vitro permeability model for human vaginal mucosa, *Int. J. Pharm.* 305 (2005) 105–111. doi:10.1016/j.ijpharm.2005.09.002.
- [39] A.D. Van Eyk, P. Van Der Bijl, Comparative permeability of various chemical markers through human vaginal and buccal mucosa as well as porcine buccal and mouth floor mucosa, *Arch. Oral Biol.* 49 (2004) 387–392. doi:10.1016/j.archoralbio.2003.12.002.
- [40] B.J. Catalone, T.M. Kish-catalone, R. Lynn, E.B. Neely, M. Ferguson, C. Fred, M.K. Howett, M. Labib, R. Rando, L.R. Budgeon, F.C. Krebs, B. Wigdahl, Mouse Model of Cervicovaginal Toxicity and Inflammation for Preclinical Evaluation of Topical Vaginal Microbicides, *Antimicrob. Agents Chemother.* 48 (2004) 1837–1847. doi:10.1128/AAC.48.5.1837.
- [41] J.A. Fernández-Romero, C.J. Abraham, A. Rodriguez, L. Kizima, N. Jean-Pierre, R. Menon, O. Begay, S. Seidor, B.E. Ford, P.I. Gil, J. Peters, D. Katz, M. Robbani, T.M. Zydowsky, Zinc acetate/carrageenan gels exhibit potent activity in vivo against high-dose herpes simplex virus 2 vaginal and rectal challenge, *Antimicrob. Agents Chemother.* 56 (2012) 358–368.

## SUPPLEMENTARY MATERIALS

### *1. Peptides characterization (E2 and E2-FAM)*

E2 and E2-FAM were analyzed by ES-MS. E2 and E2-FAM have a MW of 2166 and 2522.6 respectively. Figures 1(a) and 2(a) shows a full scan of E2 and E2-FAM respectively, Figure 1(b) shows the ion products of E2 and Figure 2(b) shows UPLC chromatogram of E2-FAM

### *2. Mass spectrometry and chromatographic conditions for the HIV inhibitor peptide (E2)*

#### *2.1. HPLC UV-VIS*

The HPLC system consisted of a Waters® 515 HPLC Pump, a 717 Plus auto sampler and a 2487 absorbance detector dual (Waters, Milford, MA, USA). The analytical column was Kromasil 100 C18 column (250mm×4.6mm, 5µm, Teknokroma). The peptide was detected at a wavelength of 280 nm with a flow rate of 1.0 mL/min. The mobile phase was acetonitrile–water (95:5 v/v) and it was chosen as it gave the best peak resolution. The injection volume was 25 µL. All determinations were performed at room temperature and isocratic conditions of elution. The retention time for the samples was 15.9 min.

#### *2.2. HPLC-MS/MS*

Both the peptides and their fluorescent derivatives were analyzed by ES-MS with a liquid chromatograph-time of flight (LC-TOF). LCT Premier XE (Micromass Waters (Mildford, MA, USA), coupled to Analytical Ultra Performance Liquid Chromatography apparatus (UPLC, Waters, Mildford, MA, USA). Samples were dissolved in a mixture of acetonitrile/water (1/1, v/v) and analyzed in the UPLC at a flow rate of 0.3 ml/min. LC-MS/MS was carried out on a QTrap 6500 (Absciex) mass spectrometer integrated on an Agilent 12690 HPLC system. The column Kinetex 2.6 µm, C18 100Å 50 x 2,1 mm column was used as stationary phase. The column temperature was set at 60°C. The mobile phase consisted of a binary solvent system using water acidified with 0.1% formic acid (solvent A) and 100% acetonitrile (solvent B), kept at a flow rate of 750 µL/min. The gradient program started with 98% of eluent A and 2% of eluent B. Eluent B rose linearly to 98% in 3 min, maintaining this level for 0.6 min. At minute 5, the gradient returned to the initial conditions and the column was re-equilibrated for 3 min between injections. The mass spectrometer was calibrated so that mass accuracy specifications and sensitivity were obtained over the entire mass range. Before validation and quantification, the system was optimized to give the highest sensitivity in the detection of peptides: peptide-standards and samples, with the most suitable decluttering potential (DP) and energy collision (EC) for each peptide. All the analyses used the turbo ion-spray source in positive mode with the following settings: ion spray voltage 5500V, DP (decluttering potential 171.23, entrance potential (EP) 5.00; data were recorded in multiple reaction monitoring mode. Transitions of 1083.0/995.5 (quantization) and 1083.0/792.8 (confirmation) were selected and collision energy applied was 35.2 and 31.77 respectively (Figure 1). The retention time of

E2 peptide was at 2.2 minutes. Figure 3 shows a chromatogram obtained from peptide released from NPs.

### **3. Analytical Method Validation**

#### **3.1 Sample Preparation**

Stock solutions (0.22 mg/mL) of E2 were prepared in solution solvent (ACN: Milli Q Water and 1mM DTT (60:40 v/v). Secondary standard solutions were prepared in the matrix, (supernatant obtained of blank nanoparticles and solution solvent) at concentrations of 27.5; 45; 55; 90; 110; 180 and 220  $\mu\text{g/mL}$  for HPLC UV-VIS. Likewise, the secondary standard solutions for HPLC/MS-MS were prepared in receptor medium used as matrix, at concentrations of 1, 3, 12, 25, 50 and 100  $\text{ng/mL}$ .

Validation of the developed method was carried out as per the International Conference on Harmonization guidelines (ICH) (1). Characteristics such as linearity, selectivity and sensibility were included.

#### **3.2. Linearity and Range**

The linearity was evaluated using five calibration curves in the range from 27.5 to 220  $\mu\text{g/mL}$  on the E2 quantification by HPLC with UV detector. Four calibrated curves in the range from 1 - 100  $\text{ng/mL}$  for quantification of E2 released from nanoparticles, using HPLC-MS/MS procedure. The calibration curves were validated interday, developed by plotting the instrument measurements versus the corresponding peptide concentrations. The method of least squares fit was used to statistically evaluate the results for linearity through a regression line and the corresponding slope, y-intercept and determination coefficients ( $r^2$ ). The regression equation was calculated:  $y = bx + a$ , where x is the concentration, (y) area of the chromatographic peaks, (b) is the value of the slope and a y-intercept. Furthermore, for HPLC UV-Vis the linearity was determined with one-way analysis of variance (ANOVA), test comparing the peak areas ratio versus the concentration of each standard. In addition, a run test was used, to determine whether HPLC-MS/MS was a linear method and whether results differ significantly from a straight line. Differences were considered statistically significant when  $p < 0.05$ , regression analysis and mathematical determinations were performed by the Prism, V. 3.00 software (GraphPad Software Inc., San Diego, CA, USA).

#### **3.3. Precision and Accuracy**

Five calibration curves were used for precision and accuracy studies and seven concentration levels were evaluated for each curve

The precision expresses degree of scatter between a series of measurements. Precision was evaluated and expressed as the mean coefficient of variation (CV%).

The accuracy of the analytical method expresses the closeness between experimental results and the real results of the sample. Accuracy was obtained calculating the percentage deviation (%EE) of the concentrations observed (experimental value) from the nominal concentration (theoretical values) of each

standard, and it is reported as percentage recovery. The method was considered precise and accurate, whether confidence intervals are within  $\pm 10\%$ .

#### **3.4. Sensitivity**

Sensitivity was calculated based on the residual standard deviation (RSD) of the response and the slope. Average values of five calibration curves were used for this purpose. LOD and LOQ was calculated using the following equations, respectively.

$$\text{LOD} = 3.3 (\text{SD}/\text{Slope}) \quad (1)$$

$$\text{LOQ} = 10 (\text{SD}/\text{Slope}) \quad (2)$$

The slope (S) was estimated from the calibration curve. The standard deviation (SD) was calculated of the y-intercepts of the regression lines. Typical signal-to-noise ratio is 3.3 for LOD and 10 for LOQ.

#### **3.5. Applicability of Methods**

The proposed methods were applied to quantify the E2 peptide encapsulated into PLGA nanoparticles and released in vaginal tissues. The validation of these two methods will be used in upcoming studies for quantification of the peptide in *in-vivo* assays.

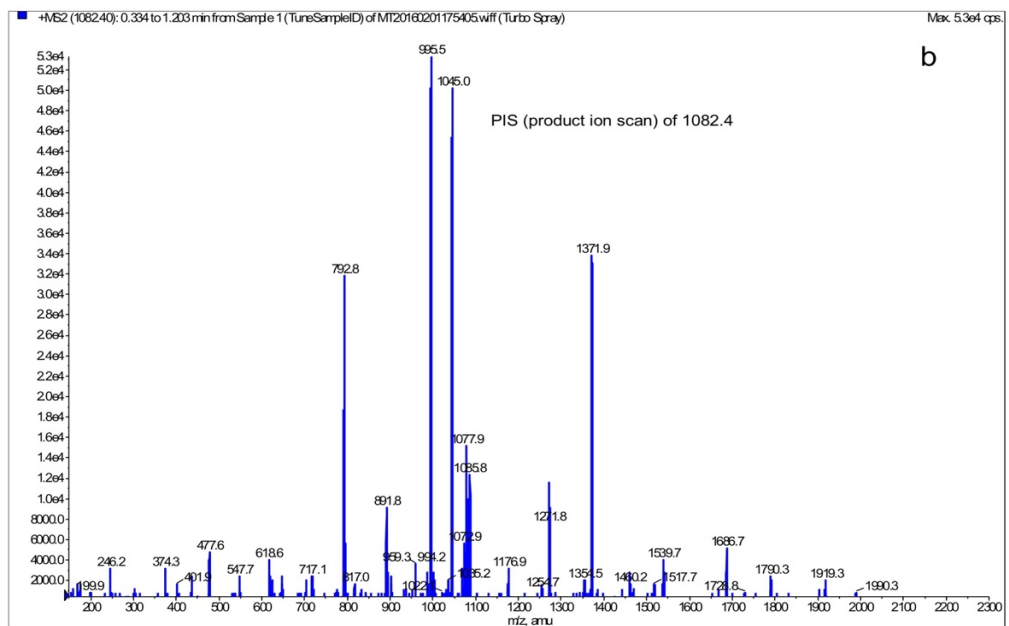
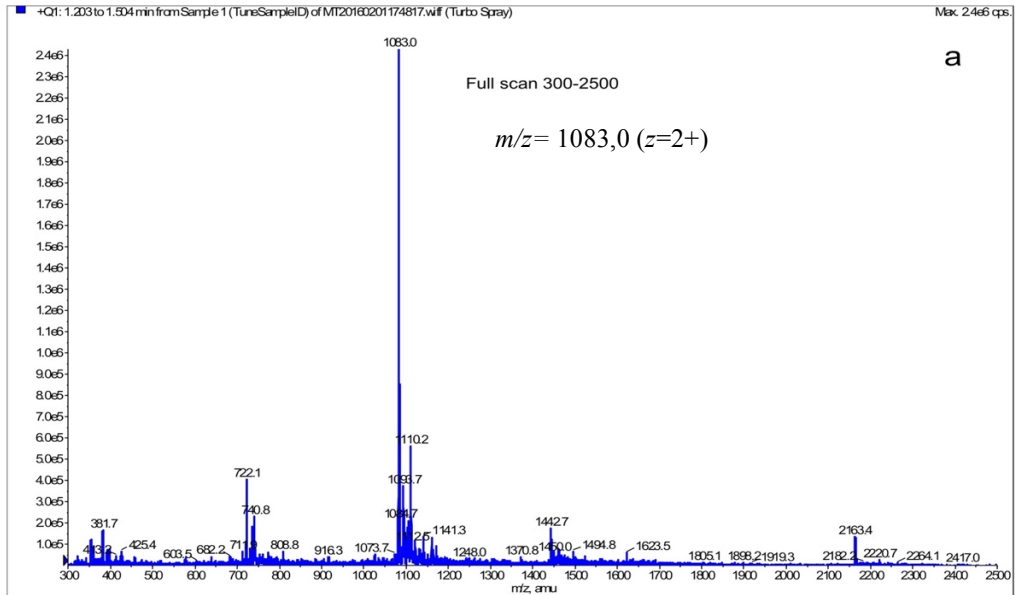


Figure 1. (a). Mass spectrum of E2 and (b). Product ion spectrum of E2 from  $m/z$  1083 at collision energy of 31.77

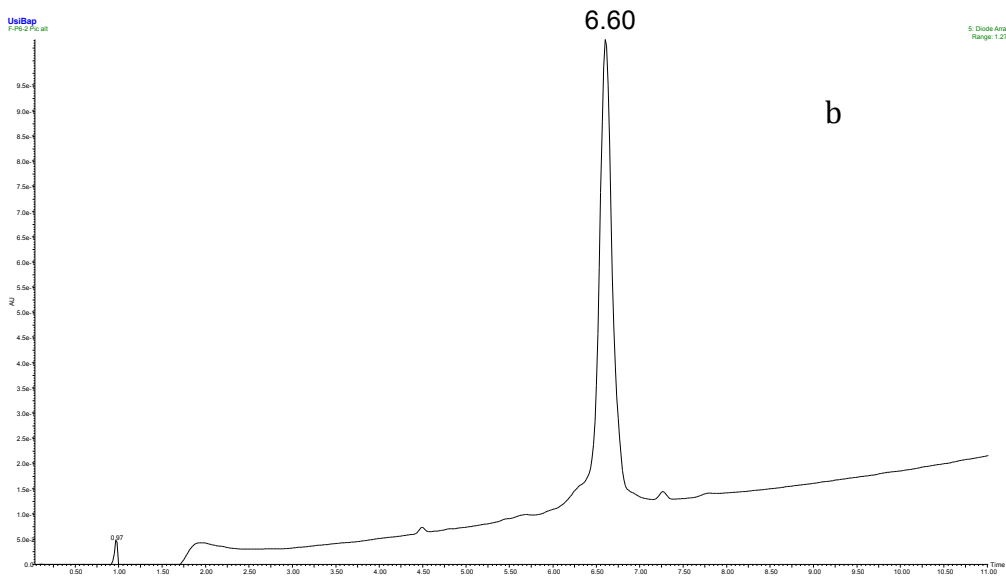
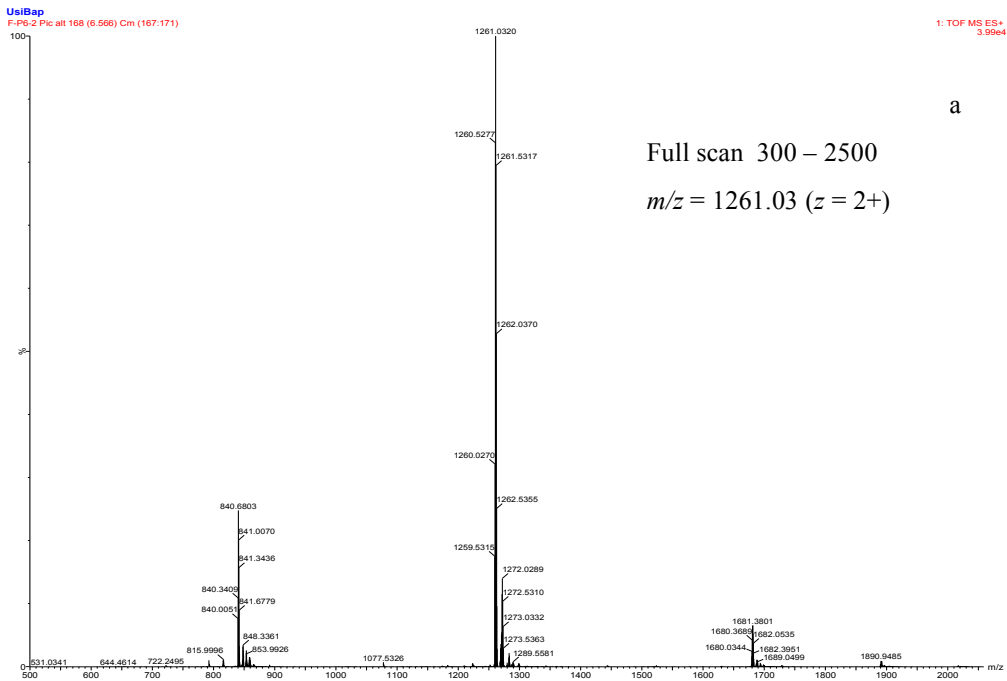


Figure 2. (a). Mass spectrum of E2-FAM and (b) UPLC- chromatogram of E2

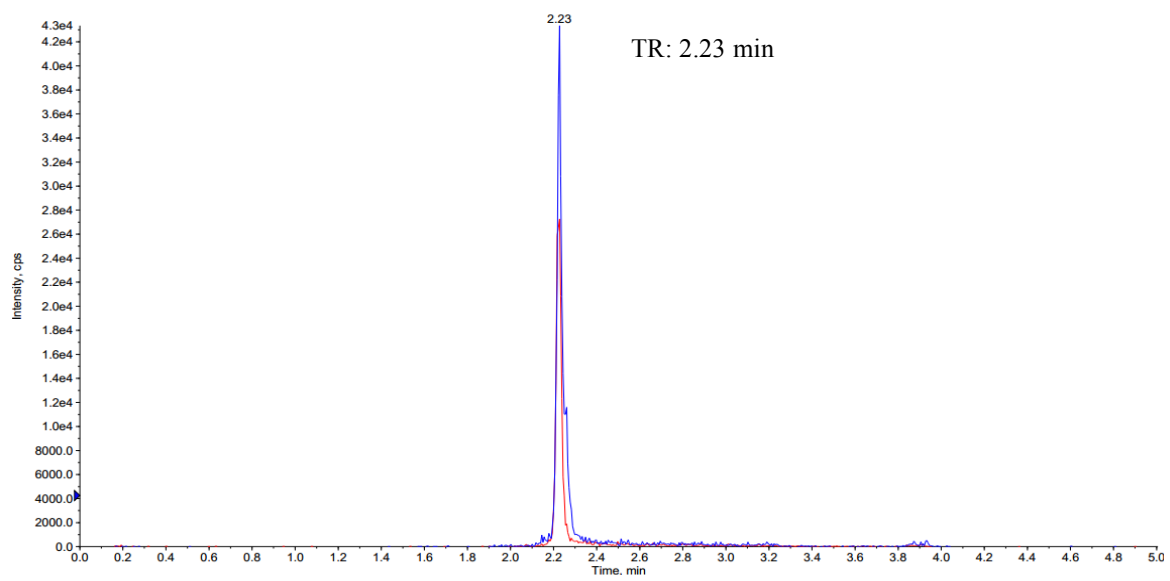


Figure 3. HPLC-MS of E2 released from NPs